# Biohybrid volatile organic compound sensing system

Elisabeth M. Steel[†‡], Zachary E. Brooks[†‡], Maegan Kornexl[†‡], Nikhil Vijai[‡], M. Aaron Hawkins[†‡], Angela Dixon[§], Mark Willis[§], Steve S. Kim[†*]
Email: Elisabeth.Steel@bluehalo.com Mark.Willis@case.edu Steve.Kim.13@us.af.mil
[†]711th Human Performance Wing, Air Force Research Laboratory (AFRL), Wright-Patterson Air Force Base, Dayton, OH, USA
[‡] BlueHalo LLC, 4401 Dayton-Xenia Rd, Dayton, Ohio, USA
[§]Department of Biology, Case Western Reserve University, 2080 Adelbert Road, Cleveland, OH, USA
*Corresponding Author: steve.kim.13@us.af.mil

***Abstract*—A biohybrid sensor is reported to integrate live insect antennae with microelectrode arrays. High resolution recording of voltage responses generated by olfactory sensory neurons (OSNs) were obtained in response to a panel of four volatile organic compounds (VOCs) at two concentrations, 20 parts per billion (ppb) and 20 parts per million (ppm). Biohybrid sensor lifetime was sustained by a novel microfluidic platform with sensor responses acquired at 24 hours, 48 hours, 7 days, and 14 days post resection of antenna from the host. VOC identity was classified by providing OSN firing rate histograms as input into a multilayer perceptron artificial neural network (MLP ANN). Biohybrid sensor response was found to be affected by anatomical location and VOC identity and thus influenced classification accuracies. Significant classification accuracies were achieved at the 24-hour and 14-day timepoints. Toluene at the 14-day timepoint elicited a unique response resulting in 100% classification at the distal anatomical location. We believe this works provides a framework for utilizing biohybrid sensing systems for VOC detection and identification.**

***Keywords—olfaction, neural network, volatile organic compounds, VOCs, chemical sensor, Low SWaP***

## I. Introduction

Currently fieldable instruments for gas analysis are large (>0.5 cubic feet), expensive (>$50,000), and slow. Hand-held devices are limited to identification of specific targets such as nitrogen oxide, oxygen, and carbon dioxide or generalized estimated concentration of total VOCs. Currently, there are no commercially available devices harnessing the rapid, selective, sensitive capabilities of biological olfaction systems due to the challenges in the bioelectronic interfacing necessary for maintaining long-term stability and environmental conditions necessary to sustain olfactory detecting elements.

Biohybrid sensor development is limited by our incomplete knowledge and understanding of the mechanisms driving the sensitivity, selectivity, and rapid millisecond response observed in olfaction as well as challenges in developing hardware and algorithms capable of decoding olfactory responses. There are many organism-level studies demonstrating the role of olfaction during insect foraging and mating behaviors [1]. Bio-inspired sensor prototypes using odorant receptors or odorant binding proteins transduce electrical signal upon detection of a single target, but sensory elements can be unstable long-term [2-4].

Historically, the prevalence of dogs used as chemical detectors demonstrates the most practical application of leveraging olfaction in the real-world; however, there are limitations in locations for use, time of optimal arousal and effective detection states, as well as the cost of training and maintenance of these animals and handlers [5]. Other species have been explored for use in chemical detection, but limitations prevent wide-spread application. For example, bees trained to detect explosives will not exhibit conditioned behaviors at night or under environmental conditions like fog/smoke/rain [6]. Further, depending on the animal used, recording from olfactory centers in the brain may require length surgical preparation (>90 minutes) with a low yield (2-3 neurons per recording) [7].

Traditional studies of insect olfaction with the moth *Manduca sexta (M. sexta)* have employed wires to record population level sensory neuron signaling, referred to as electroantennograms (or EAGs) or single sensillum recordings to monitor single sensory neuron activity in response to volatile organic compounds (VOCs) [8, 9]. Unfortunately, wire-based EAGs fail to provide spatial information regarding location of activated olfactory sensory neurons (OSNs), while single sensillum recordings are so localized that the number of OSNs that can be simultaneously recorded is limited [7]. Recently, triple EAG using multiple electrodes improves quantification of spatiotemporal neural activity as well as enabling an expanded range of detectable compounds [10].

The biohybrid sensor approach reported here integrates live *M. sexta* moth antennae with 32-channel silicon microelectrode arrays (MEA) for high resolution recording of voltage responses generated by OSNs when exposed to VOCs. With 300,000 OSNs per antenna and at least 63 subpopulations of OSNs sensitive and specific to different chemical classes and functional groups, combinatorial OSN activation yields the potential for unique neural signatures to be generated in response to hundreds of thousands of compounds [7,11-14]. The innovative capabilities of the biohybrid volatile organic compound sensing system (B-VOSS) reported here include: (1) Spatial mapping of OSN activity in response to VOC exposure, (2) a 3-D printed microfluidic platform that maintains the antennal organ function after its removal from the host for up to two weeks, and (3) a VOC identification algorithm utilizing a multilayer perceptron artificial neural network (MLP ANN).

NAECON 2024 - IEEE National Aerospace and Electronics Conference | 979-8-3503-6762-1/24/$31.00 ©2024 IEEE | DOI: 10.1109/NAECON61878.2024.10670636

## II. Predicting VOC Identity from Olfactory Sensory Neuron Activity

### A. Mechanism of Olfaction

Discrete subpopulations of *M. sexta* antennal OSN subpopulations express one of 63 types of olfactory receptors (OR) sensitive and selective to different chemical classes [12]. The number and distribution of OSNs expressing each OR over the antenna is unknown [12]. Theoretically, a single antenna could resolve hundreds of thousands of compounds based on combinatorial coding of OSN sensing elements ($2^{63}$ ORs) [7]. The *M. sexta* antenna is an olfactory organ approximately 25 millimeters (mm) long and 1 mm in diameter with a keyhole shaped cross-section comprised of approximately 88 segments from which extend hair-like structures called sensilla which contain 2-3 neurons each, totaling almost 3500 neurons per segment [14]. OSN activation occurs via ligand-gated OR ion channels which result in ion influx through the OSN membrane and subsequent voltage signal transduction through the olfactory nerve to the brain [15]. The approach here to record OSN voltage responses from the primary sensory tissue using an MEA provides unique fundamental knowledge of the distribution and differential response of OSNs based on spatial mapping of odor sensitivity by measuring neuron activity.

### B. Maintaining Antennal Organ Viability During VOC Sensing

A 3-D printed microfluidic platform was developed to increase biohybrid sensor lifetime from 2 hours (unsupported) to 2 weeks (n = 3 antennae) (Fig. 1B, right). The microfluidic platform serves two key functions: (1) as a bioreactor to sustain antennal organ olfactory function and (2) as a controlled testing chamber for VOC exposure. Ports in the front of the platform provide access to the proximal end of the antenna for insertion of multichannel electrode arrays beneath the antenna lumen, positioning the recording sites alongside the antennal nerves. The MEA captures continuous voltage response over time from the axons of OSNs bundled into the olfactory nerves. The platform features an open-air testing channel through which the antenna is suspended (10 mm), while the antenna's proximal and distal ends (4 mm) are embedded within a hydrogel matrix saturated with insect media to enable perfusion of nutrients and waste exchange. A custom olfactometer enabled automated VOC delivery to multiple antennae simultaneously through the 3-D printed platform channel using custom control software which actuates the opening and closing of solenoid valves and the flow rates of mass flow controllers in combination with a photoionization detector (PID) to validate VOC concentration. A panel of 4 individual VOCs were exposed to an antenna integrated with 32-channel silicon linear MEAs with 100-micron electrode spacing (NeuroNexus, A1x32-Edge-10mm-100-177, 50 micron thickness) at 20 parts per billion (ppb) and 20 parts per million (ppm) concentrations for ten trials for each condition, with raw voltage response recordings encompassing the 200 millisecond (ms) stimulus and recovery period (2 minutes total). The data acquisition

Funded Sources: LRIR, Air Force Office of Scientific Research
LUCI, The Undersecretary of Defense

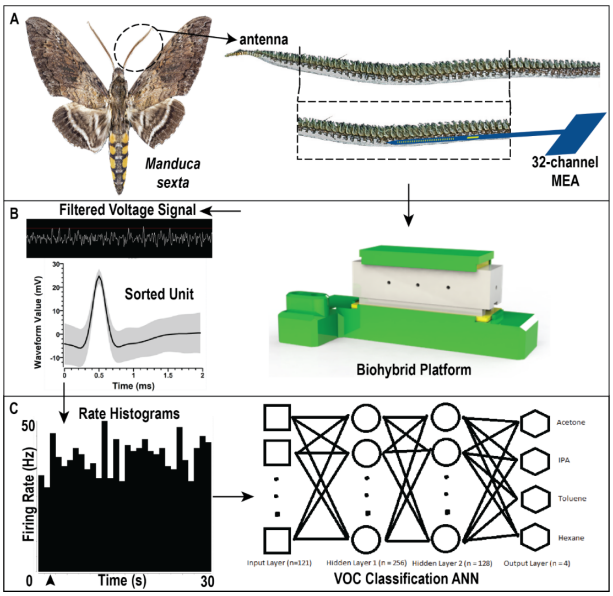


Fig. 1. (A) An antenna from *Manduca sexta* is trimmed and integrated with a 32-channel microelectrode array for electrophysiological detection of olfactory sensory neuron activity. (B) The antenna and MEA are integrated with a microfluidic device to create a biohybrid sensing platform capable of sustaining neuron viability and serving as an air flow testing chamber for volatile organic compound (VOC) exposure. Voltage signals are collected from the biohybrid sensor, filtered, and sorted into neural units using principal component analysis. Each channel's neural activity is converted into (C) firing rate histograms that signify how many times the neural unit depolarized per second in response to VOC exposure (arrowhead). Firing rate histograms from the data set serve as inputs into a classification ANN to learn the association between firing rate patterns and VOC stimuli resulting with the VOC classification as the output.

system and software were NeuroNexus Smartbox Pro and Radiens software suite (30 kHz sampling rate). VOC stimulus was generated by passing house air over the headspace of 1 milliliter (ml) of each VOC, controlled by a mass flow controller using a flow rate validated for each VOC to generate a vapor at concentrations of 20 ppb or 20 ppm as measured by the in-line PID (Ametek VOC-TRAQ II). The VOC panel consisted of toluene, acetone, isopropyl alcohol (IPA), and hexane (Sigma Aldrich). Data recordings were collected at 24-hour, 48-hour, 7-day, and 14-day timepoints from antenna harvest and platform set-up.

### C. Data Reduction of Olfactory Sensory Neuron Voltage Responses

Raw voltage signals (Fig. 1B, left) were acquired and stored prior to processing and analysis. Each 2-minute trial of voltage-time series data using the NeuroNexus Radiens Curate package was converted to Plexon file format for waveform detection by thresholding at ±3σ of baseline signal, followed by automated spike sorting in Plexon Offline Sorter software. Waveform detection parameters included a 1.5 millisecond (ms) window, and the spike sorting algorithm used K-means PCA with 2 to 15 seeds. The data clusters resulting from spike sorting indicated the presence of multiunit activity rather than clearly defined clusters indicative of single unit activity (where unit refers to

"neuron"). Therefore, to standardize the data across channels for input into an artificial neural network, the automatically sorted units were merged into one for each channel. An example of three units merged into one is shown in Fig. 1 B, where the solid line indicates the mean, and the grey shaded region indicates the standard deviation of the voltage-time features for the waveforms identified from the original signal. Firing rate histograms were generated in Plexon NeuroExplorer software for the first 30 seconds of each trial in 200 ms bins (Fig 1C, left). Custom Python scripts automated data processing within and between the NeuroNexus and Plexon software suites. Rate histograms for each electrode site of the 32-channel MEA were exported from NeuroExplorer in .csv format with each column representing an electrode site and each row representing the fire rate in hertz (Hz) in 200 ms bins from zero to 30 seconds.

All plotting and statistical analyses were performed in Origin Pro 2021 ($\alpha = 0.05$). Mean firing rates were calculated from ten trials. The baseline calculation encompassed the first five seconds prior to stimulus, while mean firing rates for the low concentration and high concentration conditions encompassed the five second interval after the start of the stimulus (which lasted for up to 500 ms depending on the VOC, or the time determined to reach the target concentration as confirmed by the PID). Mean firing rates as a function of time are visualized as bar charts in Fig. 2 for time points of 24 hours, 48 hours, 7 days, and 14 days (error bars are SD). A two-way ANOVA was performed with Factor A being VOC concentration and Factor B being timepoint. Baseline activity had no VOC present, low concentration was 20 ppb VOC, and high concentration was 20 ppm VOC. Significance is indicated by an asterisk where $p < 0.05$. While there was

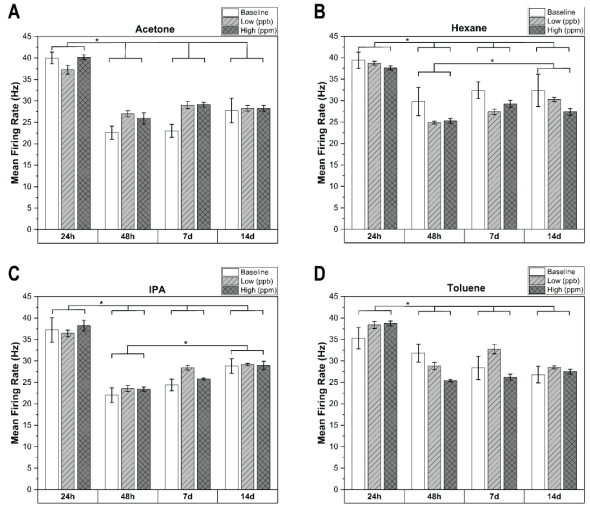


Fig. 2. Electrophysiology recordings from the most distal electrode site at 24-hour, 48-hour, 7-day, and 14-day time points were analyzed to calculate and compare the mean firing rates for 5 seconds before a VOC stimulus (baseline) and 5 seconds after a VOC stimulus at low concentration (~20 ppb) and high concentration (~20 ppm) for acetone (A), hexane (B), IPA, C), and toluene (D). A two-way ANOVA was performed for each set of VOC recordings with Factor A being VOC concentration (baseline, low, or high) and Factor B being timepoint. Significance is indicated by (*) where $p < 0.05$.

no statistically relevant main effect of VOC concentration observed on mean firing rate, the statistically significant reduction of mean firing rate over time suggests a reduction in the number of viable OSNs over time.

Fig. 3 depicts mean firing rates as a function of anatomical location, calculated from rate histograms acquired from three MEA channels located most proximal, middle, and distal along the length of the MEA spanning 3.2 millimeters (mm). These channels were spanning the center of the antenna exposed to the air channel in the testing scheme. A two-way ANOVA was performed with Factor A being VOC and Factor B being anatomical position (* = $p < 0.05$). The hypothesis at the onset of experimentation was that unique neural signatures would be generated by OSN populations in response to each VOC stimulus. Even with simplifying the neural activity to the mean firing rate, statistically significant responses occurred between different anatomical locations, with some VOCs eliciting a statistically meaningful difference in firing rate at some timepoints. For example, toluene at Day 7 elicited a greater firing rate response than other volatiles at the 20 ppm concentration. Compared to earlier timepoints, this response may be due to the presence of a sensitive OSN subpopulation being viable in excess to other subpopulations at this timepoint.

### *D. Artificial Neural Network for VOC Classification*

The driving hypothesis of biohybrid VOC sensing is that unique voltage responses will be generated by each VOC stimulus due to the differential expression of olfactory receptors by OSN subpopulations with varying VOC sensitivity and selectivity. Firing rate histograms were chosen as the input metric of OSN activity for an Artificial Neural Network for VOC classification. Further, we hypothesized that firing rate histograms would be different depending on the VOC stimulus and the anatomical location from which the sensor response was collected.

A multilayer perceptron artificial neural network (MLP ANN) programmed in *pytorch* was trained and tested at a 20:80 split after performing hyperparameter tuning through a grid search (Scikit-learn). The architecture (Fig. 1 C, right) comprised of an input layer (n=121), hidden layer 1 (n=256), hidden layer 2 (n=128) and an output layer (n = 4 classifiers, either acetone; isopropyl alcohol, IPA; toluene; or hexane). Performance modifications to reduce overfitting and slow convergence included the use of a multi-label classification method in addition to a 20% dropout technique. Training and test loss (data not shown) as well as percent classification were used to assess the goodness of fit of the ANN model for VOC classification.

Fig. 4 displays the percent accuracy in VOC classification when using rate histograms as a metric of OSN voltage response to VOC exposure. Proximal, middle, and distal labels designate the anatomical position of three representative electrode sites along the length of the antenna from which data was collected. Ten iterations of the ANN model were run, with the resulting classification represented as a point on the box plot. The bars of each boxplot visualize the 25%-75% quartiles, the line represents the median, the

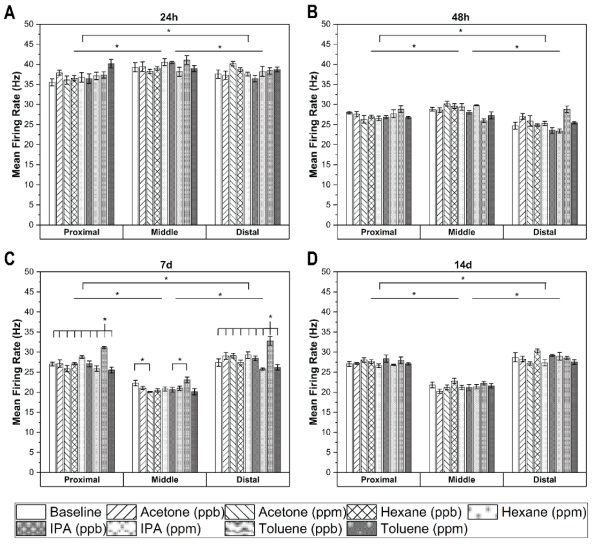


Fig. 3. Mean firing rates reported from each of three sites located most proximal, middle, and most distal along the length of the MEA spanning 3.2 mm. A two-way ANOVA was performed for each set of VOC recordings with Factor A being VOC identity and Factor B being anatomical position (proximal, middle, or distal). Significance is indicated by (*) where $p < 0.05$.

open diamond represents the mean, solid diamonds are outliers, and the bars representing the interquartile range (IQR) or range of the middle half of the data set. When the distribution of points is skewed (example seen for acetone at 24 hours low and high concentrations), outliers are defined as being 1.5 times (1.5 IQR) above or below the third and first quartiles, respectively [16].

A 2-Way ANOVA was performed to determine the effects of VOC stimulus (Factor A) and anatomical location (Factor B) on the ANN output of classification accuracy. Statistical analysis revealed a significant interaction effect between the factors of anatomical location and VOC identity on the classification accuracy of B-VOSS signals acquired at the 24-hour timepoint for 20 ppb stimuli ($p = 0.02$). While there was no main effect of VOC stimulus, classification accuracy was significantly affected by anatomical position ($p = 0.02$). For the 20 ppm condition, position had a main effect on classification accuracy ($p < 0.01$) with no main effect of VOC stimulus found. At 48 hours, the sensor response to 20 ppb was influenced by both VOC stimulus and position ($p < 0.01$), but the interaction between these factors was not significant. There were no significant main effects found at the 10 ppm 48-hour condition; however, position indicated a trend ($p = 0.06$). While the 7-day B-VOSS sensor responses did not result in any significant classification affected by VOC stimulus or position, the 14-day responses were significantly affected by VOC stimulus for both 20 ppb and ppm conditions ($p < 0.01$ and $p = 0.02$, respectively). Position had a significant effect on B-VOSS response ($p = 0.02$) for the 14-day 20 ppm condition. Toluene elicited a unique response resulting in 100% classification at the distal anatomical location.

## III. Conclusions and Future Work

The work presented here demonstrates the concept that high-density microelectrode arrays can be utilized within *M. sexta* antenna to measure unique olfactory sensory neuron activity in response to stimuli capable of being decoded by an artificial neural network for VOC identity. High classification accuracies of each VOC at some anatomical positions indicate the proximity of olfactory sensory neurons to that MEA recording site that are sensitive to the VOC tested. Differences in VOC classification accuracies at some positions over time indicate a change in viability of the OSN subpopulations within proximity to the recording site. Optimizing the hydrogel and media formulations could result in improvements in OSN viability over time and thus a more reproducible and predictable sensor response in the future. Further, refinement of the voltage signal processing methods and statistical analyses of such data reductions could potentially elucidate the location of OSN subpopulations with ORs sensitivities to different VOCs.

In summary, the B-VOSS has been demonstrated to support extended biosensor viability and provide OSN responses to VOCs for accurate classification of a panel of 4 VOCs at two concentrations using an MLP ANN. Future work will explore machine learning techniques for VOC classification and characterize B-VOSS response to VOC mixtures. The work here lays the foundation to further optimize classification algorithms for VOC identification and quantification. B-VOSS is customizable for a variety of applications and form factors. Such biohybrid sensing platforms would enable operators to detect and identify VOCs associated with explosives and illicit drugs, their synthesis byproducts, chemical warfare agents, biological agents, and human performance (i.e. through breath biomarkers) and detection (e.g. in search-and-rescue and recovery efforts).

## Acknowledgment

The authors acknowledge the funding from the Air Force Office of Scientific Research (AFOSR) as well as from the Office of the Undersecretary of Defense through the Laboratory University Collaboration Initiative (LUCI). The authors would like to thank Tom Daniel and Jeff Riffell for their discussion and feedback. The authors acknowledge the critical expertise, care, and husbandry of the *Manduca sexta* colony by Kim Thompson at Case Western Reserve University.

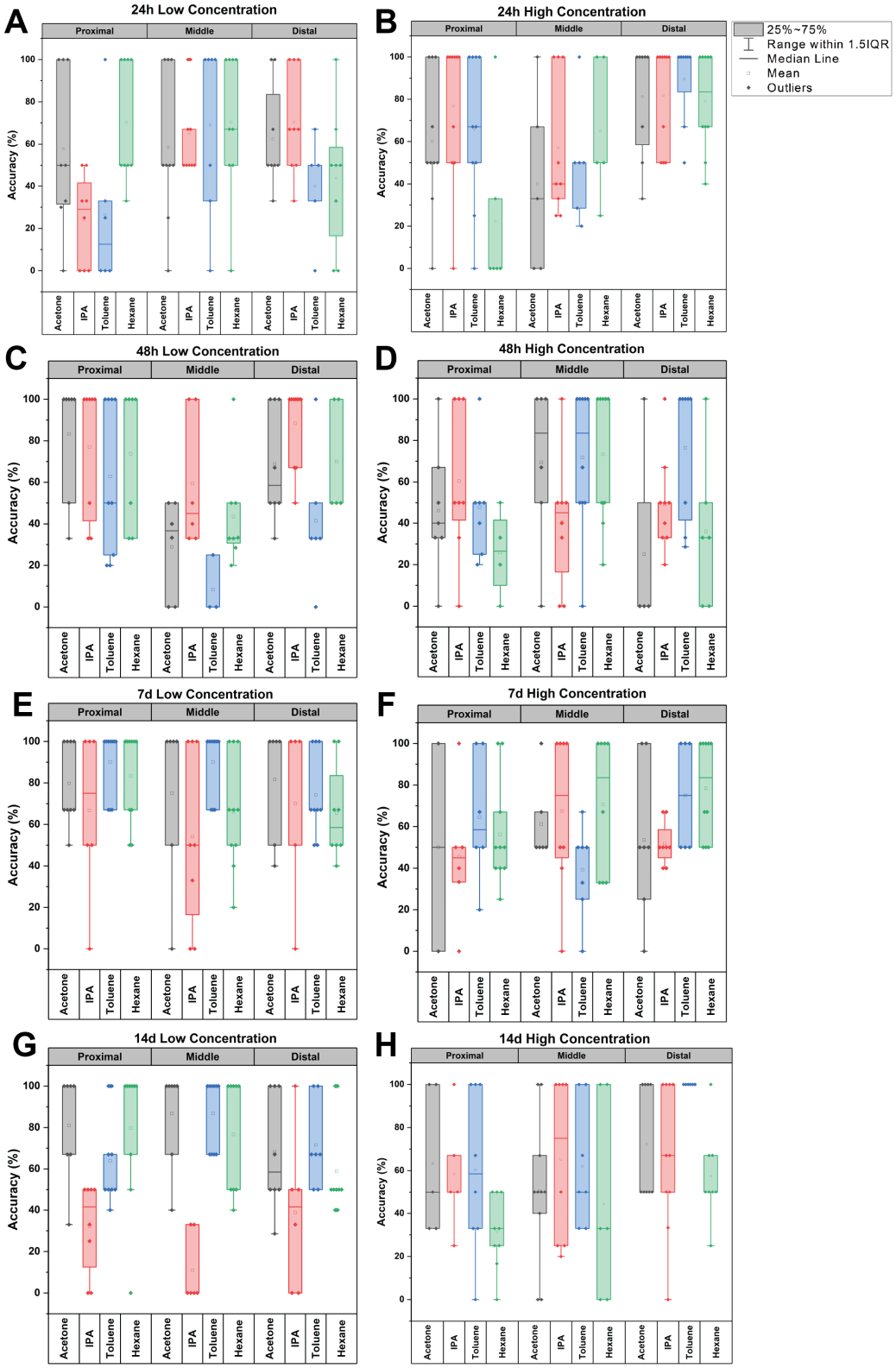


Fig. 4. Artificial Neural Network (ANN) percent accuracy in characterizing neural activity in response to volatile organic compound (VOC) exposure for low concentrations (10 parts per billion, ppb; A, C, E, G)) and high concentrations (10 parts per million, ppm; B, D, F, H) of acetone, isopropyl alcohol (IPA), toluene and hexane grouped by anatomical position (proximal, middle, distal) for voltage response recordings at 24 hours (A, B), 48 hours (C, D), 7 days (E, F), and 14 days (G, H).

## References


1. Yan, H., Jagari, S., Pask, G., Zhou, X., Reinberg, D., and C. Desplan. *Evolution, developmental expression and function of odorant receptors in insects.* Journal of Experimental Biology, 2020. 223.
2. Cheema, J.A., Aydemir, N., Carraher, C., Khadka, R., Colbert, D., Lin, H.T., Nelson, A., Kralicek, A., and A. Travas-Sejdic. *Insect odorant receptor nanodiscs for sensitive and specific electrochemical detection of odorant compounds.* Sensors and Actuators B: Chemical, 2021. 329: p. 129243.
3. Cave, J.W., J.K. Wickiser, and A.N. Mitropoulos. *Progress in the development of olfactory-based bioelectronic chemosensors.* Biosensors and Bioelectronics, 2019. **123**: p. 211-222.
4. Bachtiar, L.R., Newcomb, R.D., Kralicek, A.V. and C.P. Unsworth. *Improving odorant chemical class prediction with multi-layer perceptrons using temporal odorant spike responses from drosophila melanogaster olfactory receptor neurons*. in *2016 38th Annual International Conference of the IEEE Engineering in Medicine and Biology Society (EMBC)*. 2016.
5. Hayes, J.E., McGreevy, P.D., Forbes, S.L, Laing, G., and R.M. Stuetz. *Critical review of dog detection and the influences of physiology, training, and analytical methodologies.* Talanta, 2018. 185: p. 499-512.
6. Rodacy, PJ, S. Bender, J. Bromenshenk, C. Henderson, and G. Bender. "Training and deployment of honeybees to detect explosives and other agents of harm," Proc. SPIE 4742, Detection and Remediation Technologies for Mines and Minelike Targets VII, (13 August 2002
7. Farnum, A., Parnas, M., Apu, E.H., Cox, E., Lefevre, N., Contag, C.H., and D. Saha. *Harnessing insect olfactory neural circuits for detecting and discriminating human cancers.* Biosensors and Bioelectronics, 2023. 219: p. 114814.
8. Olsson, S.B. and B.S. Hansson. *Electroantennogram and single sensillum recording in insect antennae.* Pheromone signaling: methods and protocols, 2013: p. 157-177.
9. Ghaninia, M., S.B. Olsson, and B.S. Hansson. *Physiological Organization and Topographic Mapping of the Antennal Olfactory Sensory Neurons in Female Hawkmoths, Manduca sexta.* Chemical Senses, 2014. 39(8): p. 655-671.
10. Ramiaranjatovo, G., B. Reynaud, and V. Jacob. *Triple electroantennography captures the range and spatial arrangement of olfactory sensory neuron response on an insect antenna.* Journal of Neuroscience Methods, 2023. 390: p. 109842.
11. Tom, M.T., Cortes, L., Bucks, S., Bisch-Knaden, S., and B.S. Hansson. *Sex- and tissue-specific expression of chemosensory receptor genes in a hawkmoth.* Frontiers in Ecology and Evolution, 2022. 10.
12. Koenig, C., Hirsh, A., Bucks, S., Klinner, C., Vogel, H., Shukla, A., Mansfield, J., Morton, B., Hansson, B.S., and E. Grosse-Wilde.. *A reference gene set for chemosensory receptor genes of Manduca sexta.* Insect Biochemistry and Molecular Biology, 2015. 66: p. 51-63.
13. Shields, V.D.C. and J.G. Hildebrand. *Responses of a population of antennal olfactory receptor cells in the female moth Manduca sexta to plant-associated volatile organic compounds.* Journal of Comparative Physiology A, 2001. 186(12): p. 1135-1151.
14. Sanes, J.R. and J.G. Hildebrand. *Structure and development of antennae in a moth, Manduca sexta.* Developmental Biology, 1976. 51(2): p. 282-299.
15. Wang, Y., Qiu, L., Wang, B., Guan, Z., Dong, Z., Zhang, J., Cao, S., Yang, L., Wang, B., Gong, Z., Zhang, L., Ma, W., Liu, Z., Zhang, D., Wang, G., and P. Yin. *Structural basis for odorant recognition of the insect odorant receptor OR-Orco heterocomplex*. Science, 2024. 384, p. 1453-1460.
16. Vinutha, H.P., Poornima, B., Sagar, B.M. (2018). *Detection of Outliers Using Interquartile Range Technique from Intrusion Dataset*. In: Satapathy, S., Tavares, J., Bhateja, V., Mohanty, J. (eds) Information and Decision Sciences. Advances in Intelligent Systems and Computing, vol 701. Springer, Singapore.